Int. J. Heat Mass Transfer. Vol. 27, No. 4, pp. 611–621, 1984
Printed in Great Britain

0017–9310/84 $3.00 + 0.00

COMBINED NATURAL AND FORCED CONVECTION BETWEEN PARALLEL WALLS: DEVELOPING FLOW AT HIGHER RAYLEIGH NUMBERS

P. M. BECKETT and I. E. FRIEND*

Department of Applied Mathematics, University of Hull, Cottingham Road, Hull HU6 7RX, U.K.

(*Received* 19 *October* 1982 *and in revised form* 1 *August* 1983)

Abstract—The well-known, fourth-order, ordinary differential equation, governing vertical fully developed convection between parallel vertical walls, is discussed in the light of numerical solutions and perturbation expansions in terms of the Eckert number. The existence of multiple solutions is reaffirmed and the manner in which the various solutions grow and merge into each other with increasing Rayleigh number is established. Understanding of the structure of the solutions is aided by the study of a second-order anharmonic oscillator equation.

NOMENCLATURE

A	temperature gradient up the wall
C_p	specific heat at constant pressure
d	distance between the vertical walls
E	Eckert number, $v^2/C_p \lvert A\rvert d^3$
g	gravitational acceleration
Gr	Grashof number, $g\beta \lvert A\rvert d^3/v^2$
k	thermal conductivity
m	value of $u''(1)$, $m = 1 - Gr(T_1 - T_0)/AdQ$
p	pressure
Pr	Prandtl number, $\mu C_p/k$
Q	constant involving pressure gradient
t	time
T	temperature
T_r	reference temperature, $T_0 + AX$
T_0, T_1	wall temperatures at $X = 0$
u	dimensionless velocity, $(d/\mu Q)U$
U	physical (vertical) velocity
x	dimensionless vertical coordinate
X	vertical coordinate
y	dimensionless horizontal coordinate
Y	horizontal coordinate.

Greek symbols

β	coefficient of cubical expansion
ε	perturbation parameter, $Ra\,QE$
θ	dimensionless temperature
λ	for second-order problem, $\dot{x}(0)$
μ	absolute viscosity
v	kinematic viscosity
ρ	density
ω	in fourth-order problem, $\omega = Ra$; in second-order problem ω = frequency.

1. INTRODUCTION

THE FIRST systematic studies of convection between vertical walls, on which the temperatures vary, were presented by Ostrach [1, 2]. In the case in which the wall temperatures decrease linearly with height Ostrach showed that a simple linear model, based on a momentum balance of viscous and buoyancy forces together with a thermal energy balance between conduction and convection, predicts infinite flow rates at critical values of the Rayleigh number. Moreover, Ostrach showed that the flows either side of a critical value are of completely different character. For vertical pipes of circular section Morton [3] reached the same conclusion and introduced the phrase 'thermal runaway' to describe the rapid increase in flow rate as the Rayleigh number approaches a critical value. There is, perhaps, more physical interest in Morton's chimney problem but it is much less amenable to analytical study than the channel problem, and for that reason investigations into thermal runaway have been confined to the latter geometry. It is, however, relevant to note that the two-dimensional (2-D) model is applicable to the case of geophysical chimneys.

In his original paper [1], Ostrach modified the linear model by including viscous dissipation in order to prevent thermal runaway and presented numerical solutions of the resulting non-linear ordinary differential equation. These results not only show that the flow has a finite velocity at critical values of the Rayleigh number, but also that there are two solutions at, and near, the first critical value $Ra = \pi^4$. One solution is a Poiseuille type downflow, for which the maximum absolute velocity grows as the Rayleigh number increases through the first critical value, while the second is a Poiseuille type upflow for which the maximum velocity decreases as Ra increases. Since both solutions are stable according to linear theory (see ref. [4]) there is interest in following the development of the non-linear solutions beyond the range of Ra considered by Ostrach. The physical significance of this development may be restricted because higher flow rates would undoubtedly lead to instabilities, in addition to which several of Ostrach's basic assumptions would need reviewing; nevertheless it is of interest to discover whether there can be a continuous transition between the various linear modes via

*Present address: Marconi Space and Defence Systems, Stanmore, Middlesex.

Ostrach's non-linear equation. Moreover, analysis of this particular problem is worthwhile because it is typical of other fourth-order problems arising in convection problems (for example see ref. [5]) and also arises in the analysis of rotating shafts.

In a previous paper Beckett [6] showed that a regular perturbation expansion can yield the linear solution provided the Rayleigh number is not close to a critical value, and presented a singular expansion in the neighbourhood of $Ra = \pi^4$. The results were compared with numerical solutions up to $Ra = 150$. In this paper perturbation expansions are presented for higher critical values of Ra but the major aim is to follow the development of the various linear modes as Ra changes. In ref. [6] the behaviour of the fourth-order equation was discussed alongside that of a second-order equation which possesses striking similarities; here the second-order equation is again investigated but eventually it is the differences rather than the similarities which are emphasized.

2. FORMULATION OF THE EQUATIONS

Incompressible viscous fluid is contained between two parallel vertical infinite walls $Y = 0$ and d which are maintained at temperatures $T_0 + AX$ and $T_1 + AX$, respectively, where X is the distance measured vertically upwards. Fully developed steady 2-D flow is assumed so that the velocity is everywhere parallel to the X-axis and a function of Y alone. Under these assumptions, and invoking the Boussinesq approximation, the Navier–Stokes equation reduces to

$$\mu \frac{d^2U}{dY^2} = \left(\frac{dp}{dX} + \rho g\right) - \rho g(T - T_r), \tag{1}$$

where T_r is a reference temperature, which is taken here as $T_r = T_0 + AX$. The equation of thermal energy is

$$k\left(\frac{\partial^2 T}{\partial X^2} + \frac{\partial^2 T}{\partial Y^2}\right) = \rho C_p U \frac{\partial T}{\partial X} - \mu\left(\frac{\partial U}{\partial Y}\right)^2, \tag{2}$$

where these terms represent conduction, convection and viscous dissipation, respectively. The boundary conditions for these equations are

$$\begin{aligned} &U = 0, \quad T = T_0 + AX \text{ on } Y = 0, \\ &U = 0, \quad T = T_1 + AX \text{ on } Y = d. \end{aligned} \tag{3}$$

The system is non-dimensionalized by introducing

$$U(Y) = \frac{\nu}{d}\tilde{U}(y), \quad T(X, Y) = T_0 + AX + Ad\theta(y), \quad y = Y/d, \tag{4}$$

which yield

$$\frac{d^2\tilde{U}}{dy^2} + \operatorname{sgn}(A) Gr\, \theta = \frac{d^3}{\mu\nu}\left(\frac{dp}{dX} + \rho g\right) = Q, \text{(const.)}, \tag{5}$$

and

$$\frac{d^2\theta}{dy^2} = Pr\, \tilde{U} - \operatorname{sgn}(A) E\, Pr \left(\frac{d\tilde{U}}{dy}\right)^2, \tag{6}$$

subject to

$$\tilde{U}(0) = \tilde{U}(1) = 0, \quad \theta(0) = 0, \quad \theta(1) = (T_1 - T_0)/Ad.$$

Here the Grashof number, $Gr = g\beta|A|d^3/\nu^2$, the Prandtl number, $Pr = \mu C_p/k$, and the Eckert number, $E = \nu^2/C_p|A|d^3$.

The simultaneous equations (5) and (6) are combined to form a single equation for $u(y)$, where $u(y) = \tilde{U}(y)/Q$

$$\frac{d^4u}{dy^4} + \operatorname{sgn}(A) Ra\, u = Ra\, QE\left(\frac{du}{dy}\right)^2, \tag{7}$$

for which the boundary conditions are

$$u(0) = u(1) = 0, \quad u''(0) = 1, \quad u''(1) = m. \tag{8}$$

Here $m = 1 - Gr(T_1 - T_0)/AdQ$, $Ra = Pr\ Gr$ is the Rayleigh number and primes denote differentiation with respect to y.

In his earlier work Ostrach introduced slightly different non-dimensional variables with the result that the fourth derivative term and the non-linear term were of the same order for all combinations of the parameters. The above natural non-dimensionalization shows the viscous heating is characterized by the Eckert number, and since E is very small this term can be seen in its proper perspective; that is only at high rates of shearing is viscous dissipation a significant factor. Advantage of this was taken in ref. [6] by writing $\varepsilon = Ra\ QE$ and using ε as a perturbation parameter.

Confining interest to the case in which the temperature decreases with height (i.e. $A < 0$) leads to the equation

$$\frac{d^4u}{dy^4} - Ra\, u = \varepsilon\left(\frac{du}{dy}\right)^2, \tag{9}$$

on which the boundary conditions (8) are imposed. When $\varepsilon = 0$ this is the linear equation which predicts thermal runaway, and in particular it is a term involving $\sin(Ra^{1/4}y)$ which is responsible for the infinite velocity. Writing the differential operator $D^4 - Ra$ as $(D^2 - Ra^{1/2})(D^2 + Ra^{1/2})$ it is clear that the second factor is responsible for the difficulties and prompts interest in the following second-order problem

$$\frac{d^2x}{dt^2} + \omega^2 x = \varepsilon x^2, \tag{10}$$

$$x(0) = 0, \quad x(1) = 1. \tag{11}$$

The reason why this equation is of particular relevance was shown in ref. [6]. If $\varepsilon = 0$ there are similar singularities as for the convection problem whenever $\omega = n\pi$, $n = 1, 2, 3, \ldots$, but in this case it is easy to understand their existance; briefly if $\omega = n\pi$ and $\varepsilon = 0$ equation (10) describes simple harmonic motion so that $x(1) = 0$ if $x(0) = 0$, whereas the second boundary

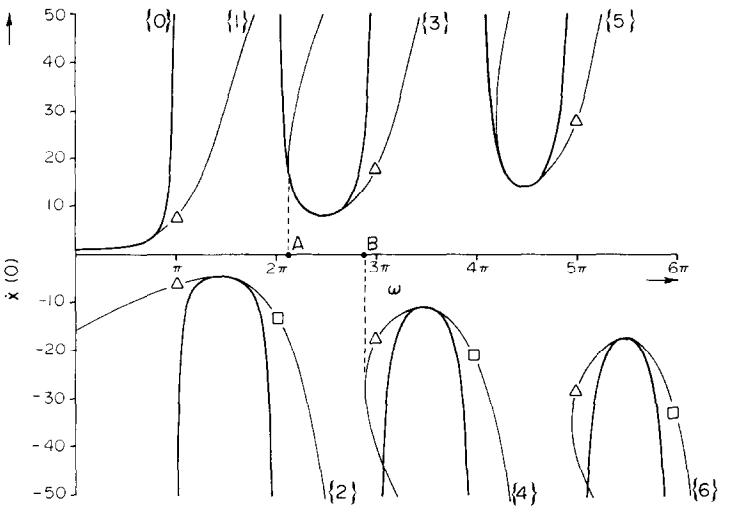

FIG. 1(a). Qualitative comparison of the zero-order function and the non-linear solution for relatively 'small' values of $\dot{x}(0)$ for the second-order problem.

condition requires the oscillator to have some other position, i.e. $x(1) = 1$. Furthermore, if ε is small, but non-zero, the same sort of expansions exist for equations (10) and (11) as for equations (9) and (8), but in this case it is possible to prove their validity because they are the limiting forms as $\varepsilon \to 0$ of the exact solution (in terms of elliptic integrals) of equation (10). Finally, if the solution of equations (8) and (9) is characterized by $u'(0)$ and that of equations (10) and (11) by $\dot{x}(0)$, the development of $u'(0)$ with Ra closely resembles the development of $\dot{x}(0)$ with ω near the first singularity $\omega = \pi$.

3. QUALITATIVE ANALYSIS OF THE SECOND-ORDER SYSTEM

Attention is focused on equation (10) subject to equation (11); as in ref. [6] $\dot{x}(0)$ is used to characterize the solutions. If $\varepsilon = 0$ the solution is

$$x(t) = \sin \omega t / \sin \omega, \tag{12}$$

providing ω is not an integer multiple of π, and then

$$\dot{x}(0) = \omega / \sin \omega. \tag{13}$$

This dependence of $\dot{x}(0)$ on ω for $\varepsilon = 0$ is shown in Fig. 1(a) as the disjoint sections labelled $\{0\}$; the sections have vertical asymptotes at $\omega = n\pi$. For small but non-zero values of ε there is a solution which is very close to the zero-order solution (i.e. with $\varepsilon = 0$) in the interior of each interval $[n\pi, (n+1)\pi]$ but which differs significantly for values of ω near the end points of each interval. The dependence of $\dot{x}(0)$ on ω for $\varepsilon \neq 0$ is also shown in Fig. 1(a), as indicated by the feinter curves $\{1\}$–$\{6\}$.

The qualitative behaviour of the odd numbered upper branches apart from $\{1\}$ are identical. As $\omega \to (2n+1)\pi$, with ω increasing, the value of $\dot{x}(0)$ obtained from numerical integration is in each case less than the value predicted by the zero-order solution; moreover, at $\omega = (2n+1)\pi$ the values of $\dot{x}(0)$ are finite and the branches extend into the adjacent interval. However, as $\omega \to 2n\pi$, with ω decreasing, the value of $\dot{x}(0)$ when $\varepsilon \neq 0$ is larger than the corresponding value for the zero-order

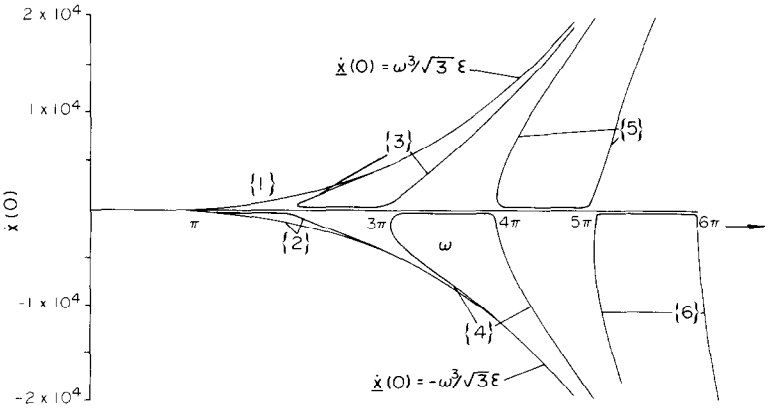

FIG. 1(b). Illustration of the asymptotic forms of branches $\{1\}$–$\{6\}$ of Fig. 1(a), $\varepsilon = 0.1$.

solution, and the branch $\{2n+1\}$ becomes vertical for a value of ω slightly larger than $2n\pi$ and then bends around to give $\dot{x}(0)$ growing as ω increases. The behaviour of branch $\{1\}$ is similar to the other upper branches towards the RHS of the interval $[0, \pi]$ but does not turn vertically upwards as $\omega \to 0$; instead this branch extends back to $\omega = 0$.

Likewise the nature of the lower even numbered branches, except for $\{2\}$, are similar to each other. As $\omega \to 2n\pi$ the value of $|\dot{x}(0)|$ is less than the linear value and the branch $\{2n\}$ remains finite at $\omega = 2n\pi$ and extends into the adjacent interval. However, as $\omega \to (2n-1)\pi$, with ω decreasing, the value of $|\dot{x}(0)|$ is again less than the zero-order value and the branch $\{2n\}$ extends back beyond $\omega = (2n-1)\pi$ before turning vertically downwards, after which $|\dot{x}(0)|$ again increases with ω. Branch $\{2\}$ extends in a similar manner to the other even numbered branches for ω increasing but like $\{1\}$ this also extends back to $\omega = 0$ rather than turning over on itself.

It should be noted that the vertical scale in Fig. 1(a) is appropriate to the zero-order solution but the behaviour of the branches is qualitative. This is because it is impossible to choose a single vertical scale which gives a reasonable display for the zero-order characteristic and which enables all the branches to be distinguished. In particular branches $\{1\}$–$\{6\}$, even for $\varepsilon = 0.1$, are so steep that only $\{1\}$ would be at all discernable if drawn to scale. On the evidence of Fig. 1(a) it is not clear whether the branches have vertical asymptotes or extend indefinitely in the direction of increasing ω. Figure 1(b), however, shows the dependence of $\dot{x}(0)$ on ω for a much larger codomain; Fig. 1(b) is the computer-drawn graph for the case $\varepsilon = 0.1$ and shows that branches $\{1\}$–$\{6\}$ do in fact extend in the direction of increasing ω, although branch $\{1\}$ is difficult to detect since on the scale to which Fig. 1(b) is drawn it is almost co-incident with the curve $\dot{x}(0) = \omega^3/\sqrt{3\varepsilon}$.

The two curves $\dot{x}(0) = \pm\omega^3/\sqrt{3\varepsilon}$ are the asymptotes of the branches $\{1\}$–$\{6\}$ as $\omega \to \infty$. The numerical results alone justify this assertion but it is quite easy to verify as follows.

Consider the behaviour of an oscillation described by

$$\frac{\mathrm{d}^2\tilde{x}}{\mathrm{d}\tilde{t}^2} + \Omega^2\tilde{x} = \varepsilon\tilde{x}^2, \tag{14}$$

when the initial conditions

$$\tilde{x}(0) = 0, \left(\frac{\mathrm{d}\tilde{x}}{\mathrm{d}\tilde{t}}\right)_{\tilde{t}=0} = \lambda, \tag{15}$$

are imposed. This equation was briefly considered in ref. [6] where it was noted that $|\lambda| < \Omega^3/\sqrt{3\varepsilon}$ is a necessary and sufficient condition for oscillatory motion, that the motion is unbounded if $|\lambda| > \Omega^3/\sqrt{3\varepsilon}$ and that the particle tends asymptotically to rest at $\tilde{x} = \Omega^2/\varepsilon$ if $|\lambda| = \Omega^3/\sqrt{3\varepsilon}$. It is also important to recognize that as $|\lambda|$ increases (subject to the condition $|\lambda| < \Omega^3/\sqrt{3\varepsilon}$) the oscillatory motion is such that the total period increases but the time spent in the region $\tilde{x} < 0$ actually decreases.

Suppose that it is possible to find a value of λ such that the ensuing motion satisfying equation (14) also satisfies the condition

$$\tilde{x}(\omega/\Omega) = (\Omega/\omega)^2, \tag{16}$$

for any prescribed value of ω. It would then follow that the function $x(t)$, where

$$x = (\omega/\Omega)^2\tilde{x}, \quad t = (\Omega/\omega)\tilde{t}, \tag{17}$$

would satisfy equation (10) and the boundary conditions (11). The characteristic $\dot{x}(0)$ may then be deduced from the solution of equation (14) as

$$\dot{x}(0) = (\omega/\Omega)^3\lambda. \tag{18}$$

Therefore, it remains to show that it is possible to choose λ so that equation (14) can be satisfied subject to equation (16) for the various branches. Figure 2(a) shows the time histories of particles described by equation (14) in the case where $\Omega = \pi$ and $\varepsilon = 0.1$ which are relevant to branch $\{1\}$ in Fig. 1(a). When $\omega < \pi$ the solution, indicated by (i) in Fig. 2(a), is approximated by the zero-order solution and has the form of the first simple mode. As λ increases the particle histories are as shown by (ii)–(vii) and these clearly pass through points $(\omega/\pi, (\pi/\omega)^2)$ for increasing values of ω. Conversely solutions of equation (14) subject to equation (16) of this first simple type exist for increasing ω; moreover, since $\omega/\pi \to \infty$ and $(\pi/\omega)^2 \to 0$ as $\omega \to \infty$, the asymptotic problem is that of finding trajectories which pass through the points $\tilde{x} = 0, \tilde{t} = \omega/\pi$ and clearly these are achieved as $\lambda \to \pi^3/\sqrt{3\varepsilon}$. The preceding argument thus leads to the conclusion that a solution to equation (10) subject to equation (11) exists with the form of this first simple mode for all $\omega > \pi$, and that as $\omega \to \infty$ the asymptotic form of $\dot{x}(0)$ is given by

$$\dot{x}(0) = (\omega/\pi)^3\lambda = \omega^3/\sqrt{3\varepsilon}. \tag{19}$$

Figure 2(b) shows a similar diagram which is relevant to branch $\{3\}$ in Figs. 1(a) and (b) as it diverges from the zero-order solution in the interval $2\pi < \omega < 3\pi$. Again that mode stretches over a wider interval of $\tilde{t}$ as λ increases and hence applies to higher values of ω when equation (10) is considered. Again the asymptotic value of $\dot{x}(0)$ will be given by equation (19).

Figure 2(c) is a little more difficult to decipher but is relevant to branch $\{4\}$ in Figs. 1(a) and (b). Curve (i) is generated by the value of λ with the smallest absolute value ($\lambda = -362.5$) and satisfies equation (16) for $\omega = 9.4$. However, as $|\lambda|$ increases the corresponding value of ω satisfying equation (16) decreases until $\lambda \sim -1170$ after which further increases in $|\lambda|$ correspond to increasing values of ω. This confirms the detailed behaviour of branch $\{4\}$ near $\omega = 3\pi$ in Fig. 1(a).

Similar conclusions may be drawn concerning the other branches, except $\{1\}$ and $\{2\}$ when ω is decreasing. The point in these cases is that the motion is *not* necessarily the beginning of an oscillatory motion.

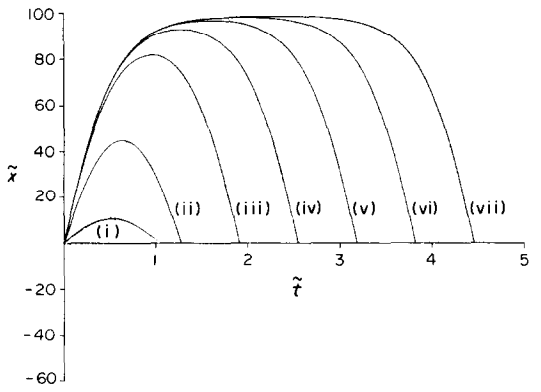

FIG. 2(a). Solutions of equation (14) subject to equation (16) for $\Omega = \pi$ and various values of ω showing first mode: (i) $\omega = 3.2$, $\lambda = 33.768$; (ii) $\omega = 4$, $\lambda = 242.40$; (iii) $\omega = 6$, $\lambda = 1197.19$; (iv) $\omega = 8$, $\lambda = 2940.57$; (v) $\omega = 10$, $\lambda = 5769.5$; (vi) $\omega = 12$, $\lambda = 9975.8$; (vii) $\omega = 14$, $\lambda = 15\,842.6$.

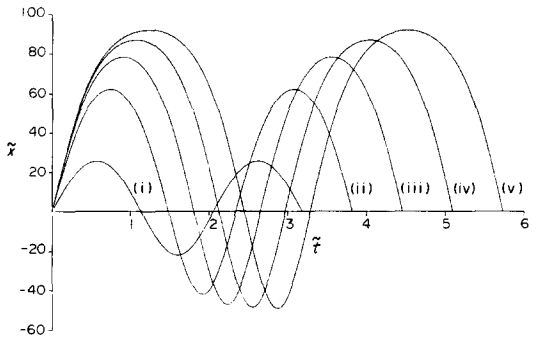

FIG. 2(b). Solutions of equation (14) subject to equation (16) showing the third mode for various values of ω: (i) $\omega = 10$, $\lambda = 2361$; (ii) $\omega = 12$, $\lambda = 8300$; (iii) $\omega = 14$, $\lambda = 14948$; (iv) $\omega = 16$, $\lambda = 22\,178$; (v) $\omega = 18$, $\lambda = 33\,436$.

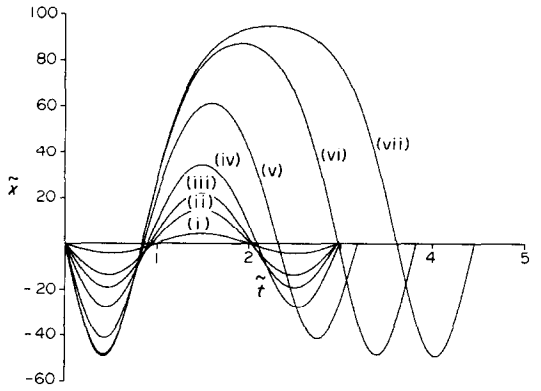

FIG. 2(c). Solutions of equation (14) subject to equation (16) showing the fourth mode for various values of ω: (i) $\omega = 9.4$, $\lambda = -362.5$; (ii) $\omega = 9.32$, $\lambda = -1172$; (iii) $\omega = 9.32$, $\lambda = -1671$; (iv) $\omega = 9.4$, $\lambda = -2531$; (v) $\omega = 10$, $\lambda = -4744$; (vi) $\omega = 12$, $\lambda = -9785$; (vii) $\omega = 14$, $\lambda = -15\,805$.

As $\omega \to 0$ the condition (16) requires the imposition of λ so that larger distances $\tilde{x}$ are attained for smaller values of time $\tilde{t}$; this is clearly possible for $\lambda > 0$ because it merely requires larger values of λ. Remembering that the time spent in the region $\tilde{x} < 0$ tends to zero as $|\lambda| \to \infty$ with $\lambda < 0$, it is equally clear that equation (16) can be also satisfied by choosing a sufficiently large negative value of λ. The existence of these solutions confirms that branches {1} and {2} in Fig. 1(a) continue back to $\omega = 0$.

4. PERTURBATION SOLUTIONS FOR THE SECOND-ORDER PROBLEM

Having successfully proved in a qualitative manner the general features in Figs. 1(a) and (b), this section is devoted to perturbation expansions which are valid in the various domains. As stated earlier, and proved in ref. [6], a solution for small ε can be obtained as a regular expansion about the zero-order solution in the interior of each interval $[n\pi, (n+1)\pi]$. In ref. [6] branch {1} was shown to have an expansion *at* $\omega = \pi$ of the form

$$x(t) = \varepsilon^{-1/2}x_{-1}(t) + x_0(t) + \varepsilon^{1/2}x_1(t) + \ldots, \quad (20)$$

and this expansion yields

$$\dot{x}(0) \sim \pm\sqrt{3}\omega^2/2\sqrt{\varepsilon}. \quad (21)$$

Attention in ref. [6] was restricted to the solution near $\omega = \pi$, but it is easy to show that expansion (20) and the resulting approximation (21) hold for all odd multiples of π. Some comparisons are listed in Table 1.

If expansion (20) is tried when ω is an even multiple of π the method breaks down due to inconsistent boundary conditions on the second perturbation function $x_0(t)$. However, it transpires that for all even multiples of π the following expansion is appropriate

$$x(t) = \varepsilon^{-2/3}x_{-2}(t) + \varepsilon^{-1/3}x_{-1}(t) + x_0(t) + \varepsilon^{1/3}x_1(t) + \ldots \quad (22)$$

Substituting equation (22) into equations (10) and (11) yields

$$x_2(t) = B \sin \omega t, \quad (23)$$

which satisfies $x_{-2}(0) = x_{-2}(1) = 0$ for any value of B. This constant is not determined until the non-homogeneous boundary conditions $x_0(0) = 0$, $x_0(1) = 1$ are imposed on $x_0(t)$, so three terms of equation (22) need to be evaluated to obtain the leading term in the expansion of $\dot{x}(0)$ compared with two terms in the case of expansion (20) at $\omega = (2n+1)\pi$. In order to determine $x_{-1}(t)$ and $x_0(t)$ it is necessary to solve for $x_1(t)$ and $x_2(t)$; although $x_{-1}(t)$ is not identically zero it does not yield a contribution to $\dot{x}(0)$ and the first correction for $\dot{x}(0)$ comes from $x_0(t)$ so that

$$\dot{x}(0) = -(12/5)^{1/3}\omega^2\varepsilon^{-2/3} - 287/255 + O(\varepsilon^{1/2}). \quad (24)$$

Comparison of this expansion with numerical results is given in Table 2.

Table 1. Comparison of numerical and perturbation approximation (21) for second-order problem

ω	ε	$\sqrt{3\omega^2/2\varepsilon^{1/2}}$ (21)	$\dot{x}(0)$ +ve numerical	−ve numerical
π	0.1	27.029	25.932	−28.309
π	0.001	270.29	269.14	−271.45
3π	0.1	243.26	233.96	−255.67
3π	0.001	2432.6	2422.3	−2443.1
5π	0.1	675.73	649.46	−708.12
5π	0.001	6757.3	6728.6	−6786.5

Further it can be seen that expansion (22) yields only one value of $\dot{x}(0)$ at $\omega = 2n\pi$ compared with two values from expansion (20) at $\omega = (2n+1)\pi$. This is entirely consistent with the qualitative observations in the previous section. The solutions given by the $\varepsilon^{-1/2}$ expansions are denoted by open triangles in Figs. 1(a) and (b), and those by the $\varepsilon^{-2/3}$ expansion by open squares. As the branches extend into adjacent regions, with the exception of $\{1\}$ and $\{2\}$ as $\omega \to 0$, then larger values of $\dot{x}(0)$ are noted and the following type of expansion becomes relevant

$$x(t) = \varepsilon^{-1}x_{-1}(t) + x_0(t) + \varepsilon x_1(t) + \ldots \qquad (25)$$

In this case no analytical progress is possible because the leading function $x_{-1}(t)$, satisfies equation (10) with $\varepsilon = 1$. However, now the equation is subject to the boundary condition $x_{-1}(0) = x_{-1}(1) = 0$ which means the non-linear oscillation returns to the origin at time $t = 1$. Such a motion would yield $\dot{x}_{-1}(0) = \dot{x}_{-1}(1)$ and moreover, since $x_{-1}(1-t)$ is a solution whenever $x_{-1}(t)$ is a solution, it is possible to deduce that in the regime when $\dot{x}(0) \sim \varepsilon^{-1}$ the solutions will occur in pairs. The values of $\dot{x}(0)$ for each pair will have the same magnitude but different sign and each solution will be the reflection of its partner about $t = 1/2$. This explains the symmetric nature of the branches, for example the LHS of branch $\{4\}$ and the RHS of branch $\{3\}$, in Fig. 1(b) away from the ω-axis.

Finally we can deduce the number of solutions of the system (10) and (11) which exist for any value of ω. Figures 1(a) and (b) show there are two solutions if $\omega \in [0, 2\pi]$; indeed ω needs to increase slightly above 2π, to the point indicated by A on Fig. 1(a), at which value of ω two solutions of the third mode are also possible. Two further solutions are augmented when ω reaches the value indicated by B; note that this also is within the interval $[2\pi, 3\pi]$. No new solution types are encountered within $[3\pi, 4\pi]$ and thereafter the pattern is repeated with four new solutions becoming possible as ω increases through each interval $[2n\pi, (2n+1)\pi]$ and none through $[(2n+1)\pi, 2n\pi]$. Thus it is possible to conclude that there are $4n-2$ solutions throughout each interval $[(2n-1)\pi, 2n\pi]$ and that the number of solutions increases within $[2n\pi, (2n+1)\pi]$ from $4n-2$ to $4n$ and thence to $4n+2$.

As an illustration of the several solutions of equation (10) subject to equation (11), Fig. 3 shows the six modes at $\omega = 10$ for $\varepsilon = 0.1$. The previously described pairs of solutions are clearly identifiable. It is important for comparison with the fourth-order problem to emphasize that each of the modes (i)–(vi) grows from a basic mode, which is almost the linear mode, within an interval $[n\pi, (n+1)\pi]$ and that the general shape is unchanged when compared to the basic mode.

Table 2. Comparison of numerical results and perturbation approximation (24) for second-order problems

ω	ε	$\dot{x}(0)$ $-(12/5)^{1/3}\omega^2\varepsilon^{-2/3}$ (24)	numerical
2π	0.1	−245.34	−244.06
2π	0.001	−5285.6	−5284.3
4π	0.1	−981.349	−980.07
4π	0.001	−21 142.0	−2114.1
6π	0.01	−2208.0	−2206.8
6π	0.001	−47 571.0	−47 569.0

5. QUALITATIVE ANALYSIS OF THE FOURTH-ORDER PROBLEM

Attention here is focused on equation (9) and the boundary conditions (8); as in the earlier paper the wall shear stress $u'(0)$ will be used to characterize the solutions (though of course two conditions at $y = 0$ are necessary to specify the solution completely). The linear equation which pertains when $\varepsilon = 0$ has the solution

$$u(y) = \frac{1}{2\omega^2}\left[\cosh(\omega y) + \frac{(m-\cosh\omega)}{\sinh\omega}\sinh(\omega y) - \cos(\omega y) + \frac{\cos\omega - m}{\sin\omega}\sin(\omega y)\right], \qquad (26)$$

from which it follows that

$$u'(0) = \frac{1}{2\omega}\left[\frac{m-\cosh\omega}{\sinh\omega} + \frac{\cos\omega - m}{\sin\omega}\right], \qquad (27)$$

where $\omega = Ra^{1/4}$. The critical values at which the solution is singular are for general values of m given by $\omega = Ra^{1/4} = n\pi$, $n = 1, 2, 3, \ldots$. There are, however, two special cases; namely if $m = 1$ the solutions seem perfectly well behaved when ω is an even multiple of π, and if $m = -1$ when ω is an odd multiple of π. The dependence of u'(0) on ω for $m = 1$, 0.9, 0 and -1 is shown in Figs. 4(a)–(d). It has already been established

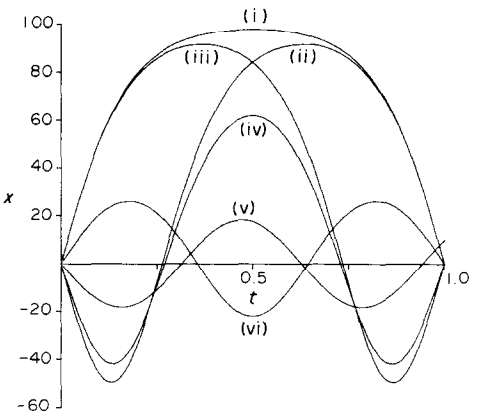

FIG. 3. The six solutions of equation (10) subject to equation (11) which exist when $\omega = 10, \varepsilon = 0.1\,(\omega^3/\sqrt{3\varepsilon} = 5.774 \times 10^3)$: (i) relevant to branch $\{1\}$, $\dot{x}(0) = 5.7695 \times 10^3$; (ii) relevant to branch $\{2\}$, $\dot{x}(0) = -5.7161 \times 10^3$; (iii) relevant to branch $\{3\}$, $\dot{x}(0) = 5.7158 \times 10^3$; (iv) relevant to branch $\{2\}$, $\dot{x}(0) = -4.7441 \times 10^3$; (v) relevant to branch $\{3\}$, $\dot{x}(0) = 2.3617 \times 10^3$; (vi) relevant to branch $\{4\}$, $\dot{x}(0) = -18.317$ (graph scaled by factor of 10^2).

that when $u'(0)$ is not large [more precisely if $\varepsilon(u')^2$ remains small compared with the linear terms] then a solution of the non-linear equation exists which is almost the same as the zero-order solution (i.e. when $\varepsilon = 0$) but that very different solutions exist when the zero-order solution predicts large enough flow rates, so that the term $\varepsilon(u')^2$ becomes significant even for very small values of ε. Conversely it might be expected that while $u'(0)$ remains small according to the zero-order approximation then the non-linear solution would be similar; in particular there would be no reason to suspect any difficulties near $\omega = 2\pi$ if $m = 1$. On the other hand if m is arbitrarily close but not actually equal to unity there is a problem. For this reason attention is initially confined to the case $m = 0.9$ and a detailed qualitative description of the way the curves in Fig. 4(b) are distorted when $\varepsilon \neq 0$. (Although $\varepsilon \sim 10^{-7}$ in the convection problem the value of $\varepsilon = 0.1$ is chosen for purposes of illustration as this leads to the same characteristics with somewhat less numerical difficulty.)

As for the second-order problem, numerical solutions are computed and Fig. 5(b) shows the results for $m = 0.9$ and $\varepsilon = 0.1$ in the range $\omega \in [0, 3\pi]$. In particular Fig. 5(b) shows that for ω close to 2π there is a deviation from the linear solution, as shown in Fig. 4(b), which is qualitatively similar to the behaviour noted in the second-order problem. That is branch $\{2\}$ in Fig. 5(b) continues beyond $\omega = 2\pi$ when $\varepsilon \neq 0$ while branch $\{3\}$ turns back on itself. It was initially thought that the behaviour noted for the second-order problem might be repeated but Fig. 5(b) shows a very different trend as ω increases for these branches. Before discussing this development though, some observations concerning the case $m = 1$ are relevant. Firstly, when $u'(0) \sim 1000$ the solution is such that an ε^{-1} expansion is valid (see Section 6) and the leading term in the perturbation is independent of m. Thus the solutions when $m = 0.9$ are virtually identical for any value of m, and in particular if $m = 1$. Thus it would be anticipated that when $m = 1$ the dependence of $u'(0)$ on ω would be virtually the same as when $m = 0.9$ except in the region of transition when the zero-order approximation is valid. It might be expected that the 'locally hyperbolic' shape shown in

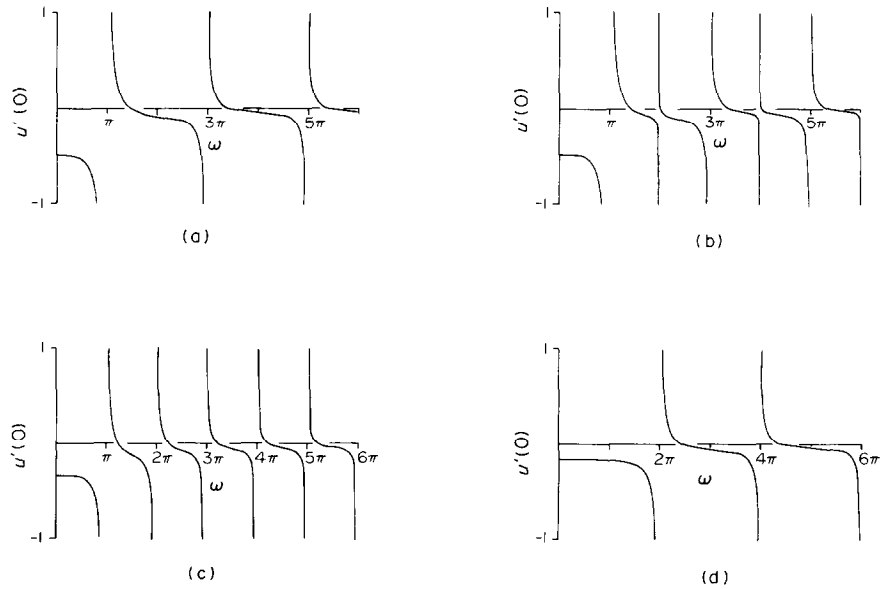

FIG. 4. The characteristic $u'(0)$ as a function of ω for the fourth-order problem with $\varepsilon = 0$: (a) $m = 1$, (b) $m = 0.9$, (c) $m = 0$, (d) $m = -1$.

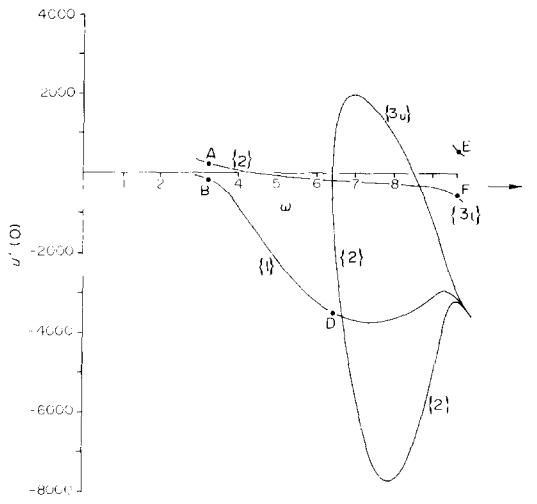

FIG. 5(a). The numerical solution of equation (9) subject to equation (8) when $\varepsilon = 0.1$ and $m = 1$.

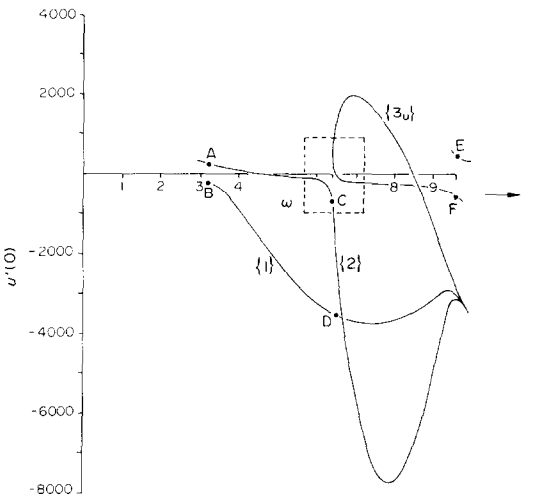

FIG. 5(b). The numerical solution of equation (9) subject to equation (8) when $\varepsilon = 0.1$ and $m = 0.9$.

the box around $\omega = 2\pi$ in Fig. 5(b) might be altered in scale as $m \to 1$ but remain of this type. However, it can be argued that in the limit when $m = 1$ the curves coalesce and give the dependence shown in Fig. 5(a) near $\omega = 2\pi$. The basis for this argument is that when $m = 1$ the equation is even and the boundary conditions are precisely symmetric so that if $u(y)$ is a solution then so is $u(1-y)$. Thus either $u(y)$ is itself a symmetric function, or if it is not symmetric then another solution exists for which $u'(0)$ has the value of $-u'(1)$ in the non-symmetric solution. Since branches $\{2\}$ and $\{3\}$ are relevant to such pairs of non-symmetric solutions they *must* both arise simultaneously, and the only way this can happen is if the 'locally hyperbolic' shape becomes the degenerate shape in Fig. 5(a). If interest is restricted to finding solutions at any value of ω then such observations are not of paramount concern, but if the development of a solution as ω increases is desired then such detail is indispensable. It is very easy to assume some sort of bifurcation when multiple solutions are encountered, as in ref. [5], but as seen here in the case of $m = 0.9$ this may not be the true behaviour.

Turning now to the way in which the branches develop as ω increases, both the cases $m = 1$ and 0.9 can be discussed together for reasons mentioned previously. The immediate observation from Fig. 5(a) [or Fig. 5(b)] is that branches $\{2\}$ and $\{3\}$ join up again and merge with branch $\{1\}$. This superficially is similar to the 2-D problem in which the branches asymptoted to either $\pm\omega^3/\sqrt{3\varepsilon}$. In that case, although the values of $\dot{x}(0)$ merged, the outline of the solutions $x(t)$ retained the features of the zero-order mode from which they grew. However, in the fourth-order problem the solutions themselves also become indistinguishable. Figures 6(a)–(d) show the development of the profiles along branches $\{1\}$, $\{2\}$, $\{3_u\}$ and $\{3_l\}$, respectively and it is evident that at the value $\omega = 9.1$ the appropriate curves on Figs. 6(a)–(c) are virtually the same. The slow solution in Fig. 6(d) remains quite different so that as ω increases through 3π there are only two identifiable solutions. It was thought that these profiles are really only the 'outer' solutions of some singular perturbation solution and that 'inner' expansions of an oscillatory manner, as discussed by Turcotte *et al.*, would distinguish these solutions. However, there is no numerical or analytical evidence of such behaviour so it is assumed that branches $\{1\}$, $\{2\}$ and $\{3_u\}$ relate to three solutions which do merge in every respect.

The qualitative behaviour for larger values of ω is a matter for further study but it is anticipated that the extra solutions that arise as ω increases would themselves merge with earlier solutions so that the number of different solutions would not increase at the same rate as for the second-order problem.

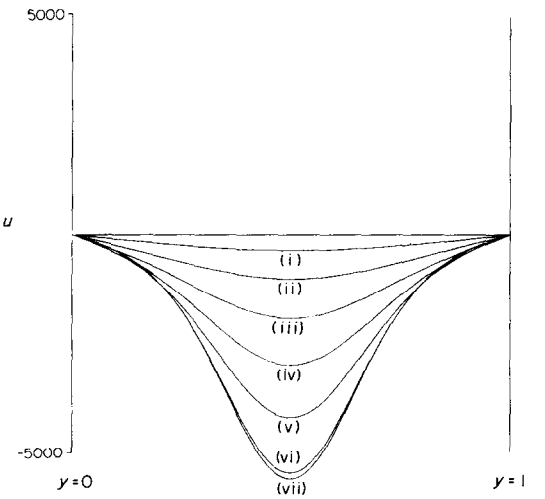

FIG. 6(a). Velocity profiles $u(y)$ for $\varepsilon = 0.1$, $m = 1$ relevant to branch $\{1\}$ in Fig. 5(a): (i) $\omega = 4$; (ii) $\omega = 5$; (iii) $\omega = 6$; (iv) $\omega = 7$; (v) $\omega = 8$; (vi) $\omega = 9$; (vii) $\omega = 9.111$.

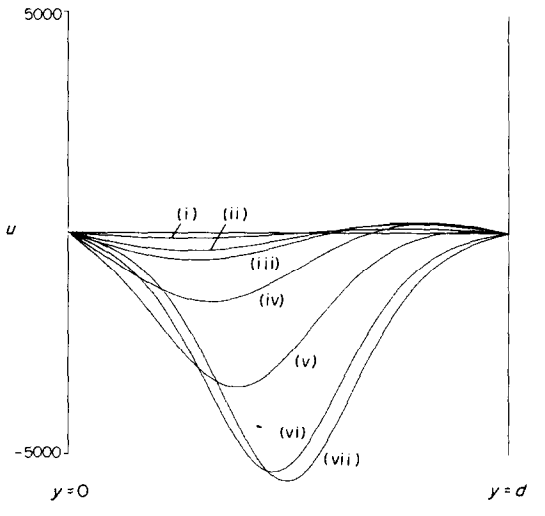

FIG. 6(b). Velocity profiles $u(y)$ for $\varepsilon = 0.1$, $m = 1$ relevant to branch $\{2\}$: (i) $\omega = 6.3$; (ii) $\omega = 6.4$; (iii) $\omega = 6.5$; (iv) $\omega = 7$; (v) $\omega = 8$; (vi) $\omega = 9$; (vii) $\omega = 9.111$.

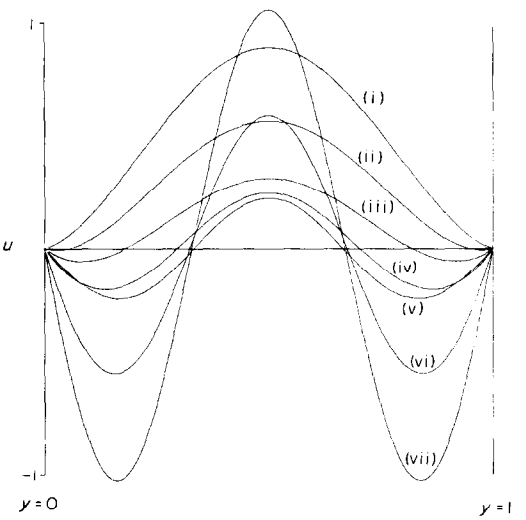

FIG. 6(d). Velocity profiles of $u(y)$ for $\varepsilon = 0.1$, $m = 1$ relevant to branch $\{3_l\}$: (i) $\omega = 4.5$; (ii) $\omega = 6$; (iii) $\omega = 7$; (iv) $\omega = 8.0$; (v) $\omega = 9.0$; (vi) $\omega = 9.4$.

6. PERTURBATION SOLUTIONS FOR THE FOURTH-ORDER PROBLEM

The simple regular expansion of the form

$$u(y) = u_{10}(y) + \varepsilon u_{11}(y) + \varepsilon^2 u_{12}(y) + \ldots, \quad (28)$$

is valid for ω on the interior of each interval $[n\pi, (n+1)\pi]$ and $u_{10}(y)$ is given by equation (26). It was further shown in ref. [6] that when $m = 1$ and $\omega = \pi$ the appropriate expansion is

$$u(y) = \varepsilon^{-1/2} u_{-1}(y) + u_0(y) + \varepsilon^{1/2} u_1(y) + \ldots, \quad (29)$$

and that this generates two solutions for which $u'(0) = \pm\sqrt{3\omega}\varepsilon^{-1/2} + O(1)$.

It transpires that equation (29) is applicable for $m \neq -1$ when ω is any odd multiple of π and that two

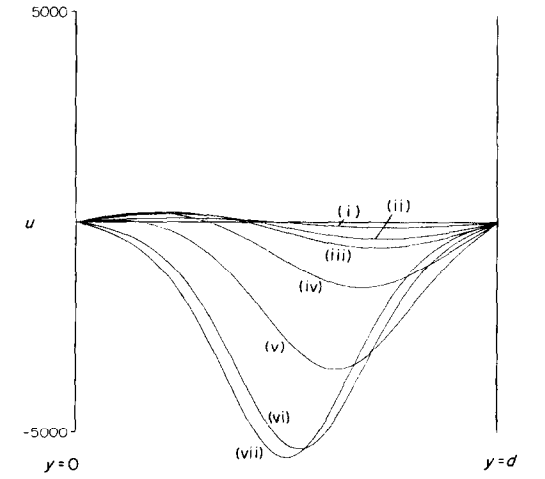

FIG. 6(c). Velocity profiles $u(y)$ for $\varepsilon = 1$, $m = 1$ relevant to branch $\{3_u\}$: (i) $\omega = 6.3$; (ii) $\omega = 6.4$; (iii) $\omega = 6.5$; (iv) $\omega = 7$; (v) $\omega = 8$; (vi) $\omega = 9$; (vii) $\omega = 9.111$.

approximations for $u'(0)$ may be deduced. Thus the values of $u'(0)$ at points A, B, E and F in Figs. 5(a) and (b) are predicted by expansion (29). [When $m = -1$ the $\varepsilon^{1/2}$ expansion breaks down but then the regular expansion (28) is valid.] The $\varepsilon^{1/2}$ expansion also fails when ω is some even multiple of π, as in the second-order problem, and for these values it is appropriate to assume

$$u(y) = \varepsilon^{-2/3} u_{-2}(y) + \varepsilon^{-1/3} u_{-1}(y) + u_0(y) + \varepsilon^{1/3} u_1(y) + O(\varepsilon^{2/3}). \quad (30)$$

After considerable algebraic labour [it is necessary to solve equations as far as $u_1(y)$ to determine $u_{-1}(y)$ completely] it follows that when $\omega = 2n\pi$

$$u'(0) = D_0 \omega \varepsilon^{-2/3} + D_1 \varepsilon^{-1/3} + O(1), \quad (31)$$

where

$$D_0 = \left[\frac{150(m-1)\omega^2 \sinh \omega}{5 \sinh \omega + 36(\cosh \omega - 1)}\right]^{1/3},$$

and

$$D_1 = \frac{D_0^2(11m-7)(1-\cosh \omega)}{30\omega(m-1)\sinh \omega}.$$

Comparison of equation (31) with the numerical calculations is displayed in Table 3 for a range of values of m and ε. No comparison is, however, made when $m = 1$ because the expansion is not valid; as in the case $m = -1$ at $\omega = (2n+1)\pi$, the regular expansion (28) holds when $m = +1$ at $\omega = 2n\pi$. For $m = 0.9$ the intersection on branch $\{2\}$ denoted by C in Fig. 5(b) is predicted by equation (31) to the accuracy shown in Table 3. As the branches extend from the region where expansion (28) applies through the region where either expansions (29) or (30) applies the values of $|\max_{y\in[0,1]} u(y)|$

Table 3. Comparison of numerical results and perturbation approximation (31) for the fourth-order problem, $\omega = 2\pi$

m	ε	numerical	$u'(0)$ $D_0\omega\varepsilon^{-2/3}$	$D_0\omega\varepsilon^{2/3} + D_1\varepsilon^{-1/3}$
0.9	0.1	−58.858	−60.214	−58.806
0	0.1	−131.351	−129.727	−131.304
−1	0.1	−166.707	−163.446	−166.665
0.9	0.001	−1290.697	−1297.272	−1290.738
0	0.001	−2802.213	−2794.889	−2802.209
−1	0.001	−3536.287	−3521.339	−3536.280

grows and the appropriate expansion is

$$u(y) = \varepsilon^{-1}\hat{u}_{-1}(y) + \hat{u}_0(y) + O(\varepsilon). \tag{32}$$

It is not possible to proceed analytically because the leading function $\hat{u}_{-1}(y)$ satisfies the same non-linear equation as $u(y)$, with $\varepsilon = 1$, but with the homogeneous boundary conditions $\hat{u}(0) = \hat{u}''(0) = \hat{u}(1) = \hat{u}''(1) = 0$. However, the numerical solutions at $\omega = 2\pi$ for $m = 1.0$, which are given in Table 4, show the dependence $u'(0) \sim \varepsilon^{-1}$ and that equation (32) is valid at D in Figs. 5(a) and (b). Unlike expansions (29) and (30) in which the leading term is not completely satisfied until subsequent terms are considered, the leading term in equation (32) is completely determined by the equation governing $u_{-1}(y)$ and the homogeneous boundary conditions on $u_{-1}(y)$. Thus the leading term is totally independent of m [if $m \sim O(1)$] and this explains why Figs. 5(a) and (b) have identical developing forms.

7. NUMERICAL TECHNIQUES

This short section is included to describe the numerical procedures which are necessary to overcome the very considerable difficulties of finding the flows with large velocities. The main algorithms are based on a fourth-order Runge–Kutta scheme and employ an iterative sequence involving shooting techniques. To initiate the iteration at any value of ω, starting guesses are required for $\dot{x}(0)$ in the second-order problem and for $u'(0)$ and $u'''(0)$ for the fourth-order problem. Some insight into the sensitivity of the fourth-order system is evident by considering the results in Table 3, which shows comparison between converged numerical solutions and perturbation approximations for $u'(0)$ when $\omega = 2\pi$. In these cases the one-term approximation for $u'(0)$ [plus a similar expression for $u'''(0)$] is nowhere near good enough to initiate a convergent sequence and the two-term approximation is necessary in every case.

While the perturbation solutions provide the necessary precision for the initial guesses for $u'(0)$ and $u'''(0)$ when $\omega = n\pi$, 'fast' solutions at other values of ω need an alternative starting strategy. In general the developments of the branches in Figs. 5(a) and (b) are obtained by advancing along the curves, in increments of ω, from a region where the linear approximation is valid. The marching is effected using cubic extrapolation from converged values of $u'(0)$ and $u'''(0)$ to generate initial estimates at each new value of ω. In Fig. 5(b) the curves are all smooth, and the marching proceeds without serious difficulty along branches $\{1\}$, $\{2\}$ and $\{3\}$ (although the ω-step needs to be greatly reduced in the neighbourhood of a critical value of ω). However, in Fig. 5(a) it is impossible to follow branch $\{2\}$ through $\omega = 2\pi$, because extrapolation leads directly onto branch $\{3_l\}$ no matter how small an ω-step is taken. However, remembering that 'fast' solutions are virtually independent of the value of m (see comment on the ε^{-1} expansion) it is possible to use values of $u'(0)$ and $u'''(0)$ for $m = 0.9$, i.e. those relevant to Fig. 5(b), as starting values for $m = 1$ on branch $\{2\}$ in $\pi < \omega < 2\pi$.

These solutions relevant to branch $\{2\}$ when $m = 1$ can also be used to generate the branch $\{3_u\}$, because $u'(0)$ on $\{3_u\}$ has the value of $-u'(1)$ which results from the solution relevant to branch $\{2\}$ (see earlier note on non-symmetric solutions in Section 5). In turn these values of $\{3_u\}$ for $m = 1$ can be used to start the iterative sequence when $m = 0.9$ and generate $\{3_u\}$ in Fig. 5(b).

8. CONCLUSIONS

Several interesting analytical aspects of the second-order problem have been presented in a manner which enhances the appreciation of the fourth-order convection problem. In particular the two problems considered together provide considerable insight into the way the basic modes are modified with increasing ω in both cases.

For the fourth-order problem it is possible to see how a fully-developed flow would behave if the Rayleigh number increased to *ca* 8000 [$\sim (3\pi)^4$], and specifically that the various flows which exist at intermediate Rayleigh numbers all develop into a single flow. In this context it is also of interest to note the nature and existence when $m = 1$ of non-symmetric solutions although the equation is even and the boundary conditions symmetric, cf. ref. [5].

Table 4. The characteristics $u'(0)$ and $u'''(0)$ from numerical solution when $\omega = 2\pi$, $m = 1$

ε	$u'(0)$	$u'''(0)$
0.1	-3.48458×10^3	-1.77089×10^5
0.01	-3.48445×10^4	-1.77080×10^6
0.001	-3.48444×10^5	-1.77079×10^7

REFERENCES

1. S. Ostrach, Combined natural and forced-convection laminar flows and heat transfer in fluids with and without heat sources in channels with linearly varying wall temperatures, NACA Tech. Note 3141, NACA, Washington, DC (1954).
2. S. Ostrach, Unstable convection in vertical channels with heating from below including the effects of heat sources and

frictional heating, NACA Tech. Note 3458, NACA, Washington, DC (1958).
3. B. R. Morton, Laminar convection in uniformly heated vertical pipes, *J. Fluid Mech.* **8**, 227–240 (1960).
4. S. Ostrach, *High Speed Aerodynamics, Vol. IV, Theory of Laminar Flows* (edited by F. K. Moore), Sect. F, Chap. 6, p. 684. Oxford University Press, London (1964).
5. D. L. Turcotte, D. A. Spence and H. H. Bau, Multiple solutions for natural convective flows in an internally heated vertical channel with viscous dissipation and pressure work, *Int. J. Heat Mass Transfer* **25**, 699–706 (1982).
6. P. M. Beckett, Combined natural and forced-convection between parallel vertical walls, *SIAM J. Appl. Math.* **39** (2), 372–384 (1980).

CONVECTION MIXTE ENTRE PAROIS PARALLELES: ECOULEMENT NON DEVELOPPE A GRAND NOMBRE DE RAYLEIGH

Résumé—L'équation différentielle classique du quatrième ordre qui gouverne la convection pleinement développée entre deux parois verticales et parallèles est discutée à la lumière des solutions numériques et des développements de perturbation en termes de nombre d'Eckert. L'existence de solutions multiples est réaffirmée et on établit la façon dont croissent les différentes solutions et se fondent l'une dans l'autre quand le nombre de Rayleigh augmente. La compréhension de la structure des solution est facilitée par l'étude de l'équation de second ordre de l'oscillation harmonique.

KOMBINIERTE FREIE UND ERZWUNGENE KONVEKTION ZWISCHEN PARALLELEN WÄNDEN: ANLAUFSTRÖMUNG BEI HÖHEREN RAYLEIGH-ZAHLEN

Zusammenfassung—Es wird die gut bekannte gewöhnliche Differentialgleichung vierter Ordnung, welche die voll entwickelte vertikale Konvektionsströmung zwischen zwei parallelen vertikalen Wänden beschreibt, hinsichtlich numerischer Lösungen und der Entwicklung nach Störungsansätzen in Abhängigkeit von der Eckert-Zahl erläutert. Die Existenz von Vielfachlösungen wird bestätigt. Es wird gezeigt, wie mit zunehmender Rayleigh-Zahl die verschiedenen Lösungen auftreten und ineinander übergehen. Das Verständnis der Struktur der Lösungen wird unterstützt durch die Untersuchung einer nichtharmonischen Schwingungsgleichung zweiter Ordnung.

СМЕШАННАЯ, ЕСТЕСТВЕННАЯ И ВЫНУЖДЕННАЯ, КОНВЕКЦИЯ МЕЖДУ ПАРАЛЛЕЛЬНЫМИ СТЕНКАМИ: РАЗВИТИЕ ТЕЧЕНИЯ ПРИ БОЛЬШИХ ЧИСЛАХ РЕЛЕЯ

Аннотация—Широко известное обыкновенное дифференциальное уравнение четвертого порядка, описывающее полностью развитую конвекцию между параллельными вертикальными стенками, исследуется с помощью численных решений и разложений возмущения по числу Эккерта. Подтверждена возможность существования множественных решений и выявлена закономерность, согласно которой различные решения растут и сливаются друг с другом с увеличением числа Релея. Для понимания структуры решений проведен анализ уравнения ангармонического осциллятора второго порядка.